EFFECT OF ROTATION ON INTERNAL SOLITARY WAVES

Karl Helfrich(1), Roger Grimshaw(2) & Ted R. Johnson(3)

(1) Woods Hole Oceanographic Institution, USA, E-mail: khelfrich@whoi.edu
(2) Loughborough University, UK, E-mail: R.H.J.Grimshaw@lboro.ac.uk
(3) University College London, UK, E-mail: e.johnson@ucl.ac.uk

The effect of rotation on internal solitary waves is explored thorough a series of laboratory experiments carried out at the LEGI-Coriolis Laboratory. The experiments confirm numerical and theoretical predictions of nonlinear wave packet formation including the packet carrier wavenumber, carrier wave phase speed and packet group speed.

1. INTRODUCTION

Internal solitary waves of large amplitudes are ubiquitous in the coastal ocean, and there have been many observations, numerical simulations and analytical studies (see Helfrich and Melville (2006) for a recent review). In this oceanic context, one key issue concerning their long-time behaviour is the role of the background earth's rotation. Although it has been known for some time that such rotation tends to convert internal solitary waves into trailing inertial-gravity waves (see the pioneering experimental work of Renouard and Germain (1994), Grimshaw et al. (1998b) and the review by Grimshaw et al (1998) for instance), the time-scale for this process and the eventual wave structure is not well understood. But recently, some numerical simulations by Helfrich (2007) for a fully nonlinear two-layer model, and by Grimshaw and Helfrich (2008) for a weakly nonlinear model, have suggested that the emergence of a wave packet with a distinctive carrier wavenumber (associated with the maximum allowed group velocity) and envelope solitary wave structure. This note reports on preliminary analysis of a recently completed set of laboratory experiments conducted at the LEGI-Coriolis Laboratory to validate these recent numerical and analytical studies which suggest an initial internal solitary wave will undergo a transformation into an envelope wave packet under the influence of background rotation.

The evolution of weakly-nonlinear, long internal waves with rotation is described by the Ostrovsky equation (Ostrovsky, 1978)

$$\left(\eta_t + \alpha\eta\eta_X + \beta\eta_{XXX}\right)_X = \gamma\eta \qquad (1)$$

here $\eta(X,t)$ is the wave amplitude and α, β, and γ are parameters of terms representing, respectively, nonlinearity, non-hydrostatic dispersion and rotation. These parameters are functions of the stratification and rotation. Here t is time, $X=x-ct$, and c is the linear long-wave phase speed. An example of a numerical solution of (1) for initial KdV solitary wave is given in Figure 1 (from Grimshaw and Helfrich, 2008). The initial solitary wave rapidly decays by radiating inertia-gravity waves. A wave packet, described by a modified Nonlinear Schrodinger equation, eventually separates from the trailing radiation. The packet is able to separate from the radiate because there is a maximum of the group velocity in linearized Ostrovsky equation at wavenumber $k_c=(\gamma/3\beta)^{1/4}$. The phase and group speeds at this carrier wavenumber are, respectively, $c = (4\beta\gamma/3)^{1/2}$ and $c_g = -(12\beta\gamma)^{1/2.}$

2. EXPERIMENTAL SETUP

The experiments were conducted using the 13 m rotating platform at the LEGI-Coriolis Laboratory in Grenoble, France. The experimental setup is shown in Figure 2. The tank was filled with a two-layer salt stratified system. The depth of the fresh upper layer h_1 = 6 cm, the depth of the slower layer h_2 = 30 cm, and the density difference of 10 ppt were fixed for all the experiments. The platform was rotated counter-clockwise (viewed from above) with period $T = \infty$, 120, 90, 60, or 45 s. The initial disturbance was produced by a dam-break from a 5 m wide by 0.45 m long (in plan view) reservoir.

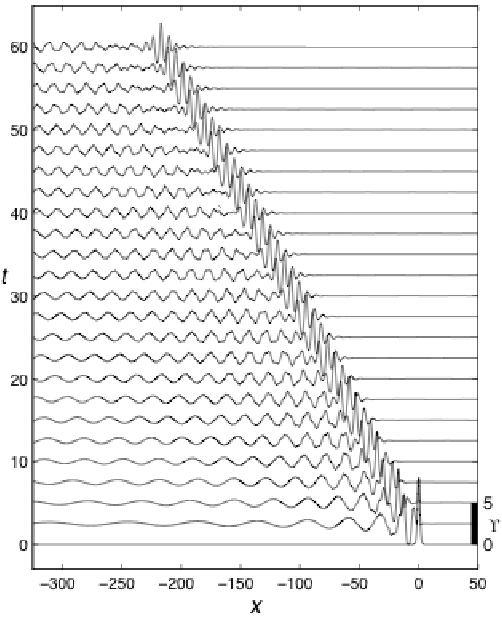

Figure 1.
Numerical solution of the Ostrovsky equation (1) (for $\alpha = \beta = \gamma = 1$) showing the formation of a leading nonlinear wave packet from an

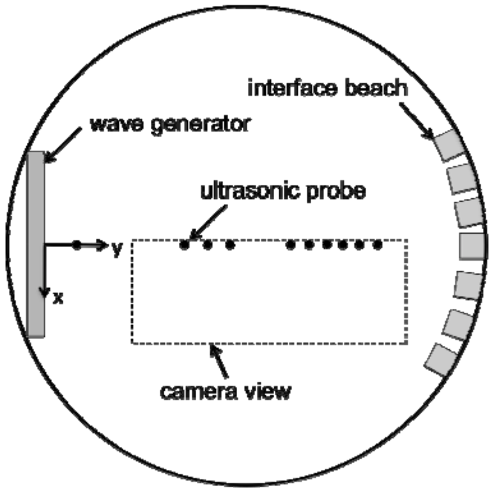

Figure 2.
Plan view sketch of the experimental setup.

The layer interface within the reservoir was lowered relative to the ambient stratification by the addition of fresh water to produce an interface elevation difference of Δh = 3, 6, 9, 12 cm. An experiment was initiated by raising the front gate of the reservoir to produce a disturbance that propagated across the tank (*y* direction) to be dissipated at a beach situated at the interface.

Measurements of the stratification inside and outside the reservoir just prior to a run were made with micro-scale conductivity-temperature probes. Measurements of the waves were made from 10 ultrasonic interface probes spaced along *y*-axis. Wave evolution in both *y* and *x* (transverse) was obtained by dying the upper layer with a water-soluble dye and imaging with three overhead CCD cameras positioned to view the area indicated in Figure 2.

3. EXPERIMENTAL RESULTS

Interface probe records from two runs with Δh = 12 cm and $T = \infty$ (non-rotating) and 60 sec are shown in Figure 3. The non-rotating experiment produced one solitary wave (and weaker trailing dispersive tail) that propagated across the tank at a nearly constant speed and with minimal amplitude decay. In contrast, rotation leads to the generation of a leading wave packet for probes located at $y > 4$ m with a clearly identifiable carrier wave period and packet group speed that is slower than the phase speed of the carrier wave. The packet structure with maximum wave amplitude behind the leading edge is characteristic of nonlinearity. Furthermore, the initial disturbance just 1 m from the wave maker already shows a packet-like structure, rather than a single solitary wave. However, there is significant evolution of the disturbance amplitude and carrier frequency between this location and the next probe at x = 4.85 m. A composite of the upper layer thickness along x = 50 cm from the overhead cameras is given in Figure 4 for a run with Δh = 9 cm and T = 60 sec. Again the packet structure is clear and both the phase and group speeds are identifiable and nearly constant.

A summary of the experimental results is given in Figure 5. The measured carrier wave length $\lambda_c = 2\pi/k_c$ (from phase speeds and wave periods in the ultrasonic records), phase speed c and packet group speed c_g are shown for the of T and Δh considered. The figure also shows the predictions for the same quantities from the linear (α = 0) two-layer Ostrovsky equation (1) computed with the experimental values and for the exact two-layer linear dispersion relation. The qualitative agreement between the theoretical predictions and the experimental data is very good. The quantitative agreement is reasonable and may improve once additional effects such as continuous stratification are incorporated into the models.

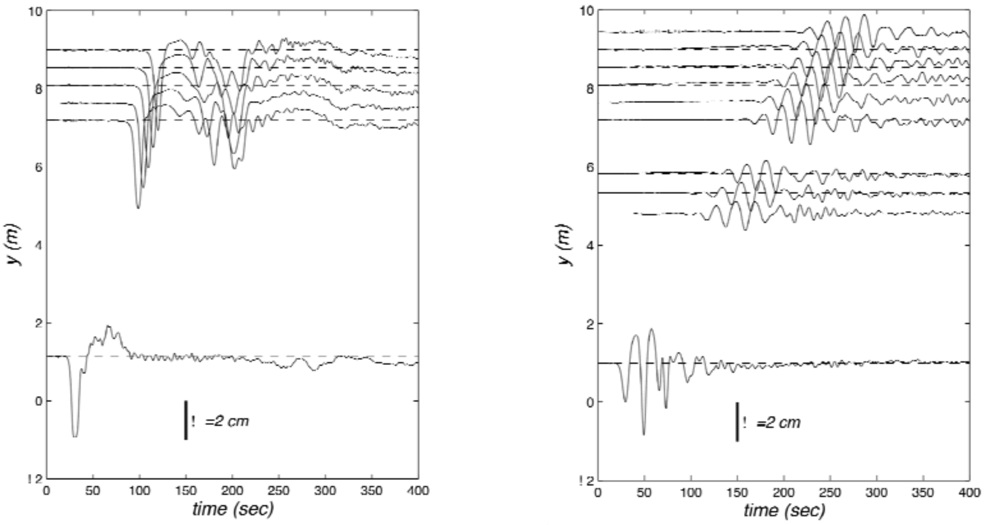

Figure 3.
Interface displacement records from two experiments with Δh = 12 cm. The LEFT panel shows a non-rotating case and the RIGHT panel shows a rotating case with T =60 s. The mean position of each record indicates the probe position in y ($y = 0$ at the wave maker gate). The interface displacement amplitude is indicated by the inset scale.

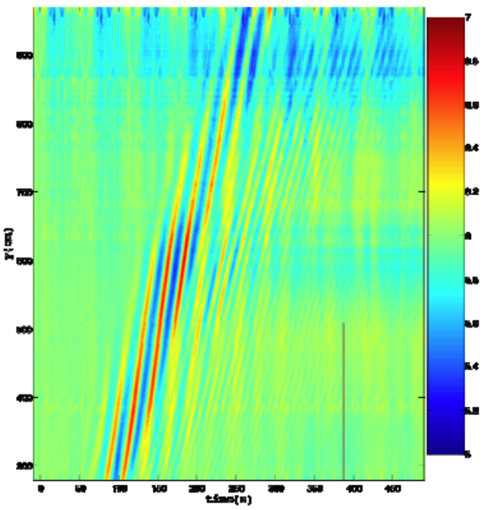

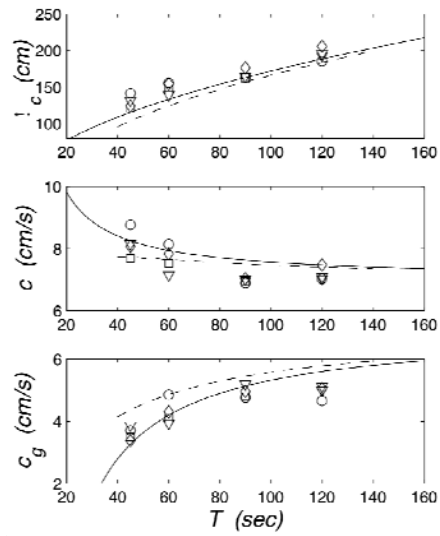

Figure 4
Upper layer thickness at x = 50 cm from the overhead cameras for an experiment with Δh = 9 cm and T = 60 s.

Figure 5.
Carrier wave length λ_c, phase speed c, and packet group speed c_g versus the rotation period T. The symbols are from the experiments with Δh = 3 cm (square), 6 (circle), 9 (triangle), 12 (diamond). The theoretical predictions from the linear two-layer Ostrovsky equation (solid) and full linear two-layer dispersion relation (dashed) are also shown.

4. SUMMARY

A preliminary analysis of experiments examining the effect of rotation on internal solitary waves shows good qualitative agreement with previous numerical and theoretical studies predicting emergence of a leading nonlinear wave packet. Future work will consider the effects of continuous stratification, wave amplitude, transverse structure, and make direct comparisons of the experimental results with nonlinear models (e.g. Ostrovsky equation and the full Euler equations).

ACKNOWLEDGEMENTS

This work has been supported by European Community's Sixth Framework Programme through the grant to the budget of the Integrated Infrastructure Initiative HYDRALAB III within the Transnational Access Activities, Contract no. 022441. KRH is supported by the US Office of Naval Research Grant N00014-0910227.

REFERENCES

Grimshaw, R., Ostrovsky, L.A., Shrira, V.I. and Stepanyants, Yu.A. 1998a. Nonlinear surface and internal gravity waves in a rotating ocean. *Surveys in Geophysics* **19**, 289-338.

Grimshaw, R.H.J., He, J-M. and Ostrovsky, L.A. 1998b. Terminal damping of a solitary wave due to radiation in rotational systems. *Stud. Appl. Math*., **101**, 197-210.

Grimshaw, R. and Helfrich. K.R. 2008. Long-time solutions of the Ostrovsky equation. *Stud. Appl. Math*. **121**. 71-88.

Helfrich, K. and Melville, W. K. 2006. Long nonlinear internal waves. *Ann. Rev. Fluid Mech.* **38**, 395-425.

Helfrich, K. 2007. Decay and return of internal solitary waves with rotation. *Physics Fluids* **19**, 026601.

Renouard, D. and Germain, J-P. 1994. Experimental Study of long nonlinear internal waves in rotating fluid. *Ann. Geophysicae* **12**, 254-264.

Ostrovsky, L. 1978. Nonlinear internal waves in a rotating ocean. *Oceanology* **18**(2), 119-125.